

World Journal of *Gastroenterology*

World J Gastroenterol 2022 July 21; 28(27): 3282-3534



REVIEW

- 3282 Hepatitis B and circadian rhythm of the liver
Skrlec I, Talapko J
- 3297 Tumor microenvironment in pancreatic ductal adenocarcinoma: Implications in immunotherapy
Smith C, Zheng W, Dong J, Wang Y, Lai J, Liu X, Yin F
- 3314 Crosstalk between dietary patterns, obesity and nonalcoholic fatty liver disease
Ristic-Medic D, Bajerska J, Vucic V

MINIREVIEWS

- 3334 Application of intravoxel incoherent motion diffusion-weighted imaging in hepatocellular carcinoma
Zhou Y, Zheng J, Yang C, Peng J, Liu N, Yang L, Zhang XM
- 3346 Regulatory T cells and their associated factors in hepatocellular carcinoma development and therapy
Zhang CY, Liu S, Yang M
- 3359 Single-incision laparoscopic surgery to treat hepatopancreatobiliary cancer: A technical review
Chuang SH, Chuang SC
- 3370 Probiotics and postbiotics in colorectal cancer: Prevention and complementary therapy
Kvakova M, Kamlarova A, Stofilova J, Benetinova V, Bertkova I
- 3383 Interventional strategies in infected necrotizing pancreatitis: Indications, timing, and outcomes
Purschke B, Bolm L, Meyer MN, Sato H
- 3398 Artificial intelligence in liver ultrasound
Cao LL, Peng M, Xie X, Chen GQ, Huang SY, Wang JY, Jiang F, Cui XW, Dietrich CF
- 3410 Risk factors and diagnostic biomarkers for nonalcoholic fatty liver disease-associated hepatocellular carcinoma: Current evidence and future perspectives
Ueno M, Takeda H, Takai A, Seno H

ORIGINAL ARTICLE

Basic Study

- 3422 Accumulation of poly (adenosine diphosphate-ribose) by sustained supply of calcium inducing mitochondrial stress in pancreatic cancer cells
Jeong KY, Sim JJ, Park M, Kim HM

- 3435** RING finger and WD repeat domain 3 regulates proliferation and metastasis through the Wnt/ β -catenin signalling pathways in hepatocellular carcinoma

Liang RP, Zhang XX, Zhao J, Lu QW, Zhu RT, Wang WJ, Li J, Bo K, Zhang CX, Sun YL

- 3455** Associations of gut microbiota with dyslipidemia based on sex differences in subjects from Northwestern China

Guo L, Wang YY, Wang JH, Zhao HP, Yu Y, Wang GD, Dai K, Yan YZ, Yang YJ, Lv J

Retrospective Cohort Study

- 3476** Prognostic significance of hemoglobin, albumin, lymphocyte, platelet in gastrointestinal stromal tumors: A propensity matched retrospective cohort study

Zhao Z, Yin XN, Wang J, Chen X, Cai ZL, Zhang B

Retrospective Study

- 3488** Contrast-enhanced ultrasound Liver Imaging Reporting and Data System: Lights and shadows in hepatocellular carcinoma and cholangiocellular carcinoma diagnosis

Vidili G, Arru M, Solinas G, Calvisi DF, Meloni P, Sauchella A, Turilli D, Fabio C, Cossu A, Madeddu G, Babudieri S, Zocco MA, Iannetti G, Di Lembo E, Delitala AP, Manetti R

- 3503** Novel index for the prediction of significant liver fibrosis and cirrhosis in chronic hepatitis B patients in China

Liao MJ, Li J, Dang W, Chen DB, Qin WY, Chen P, Zhao BG, Ren LY, Xu TF, Chen HS, Liao WJ

SYSTEMATIC REVIEWS

- 3514** Percutaneous transhepatic cholangiography *vs* endoscopic ultrasound-guided biliary drainage: A systematic review

Hassan Z, Gadour E

CASE REPORT

- 3524** Isolated gastric variceal bleeding related to non-cirrhotic portal hypertension following oxaliplatin-based chemotherapy: A case report

Zhang X, Gao YY, Song DZ, Qian BX

LETTER TO THE EDITOR

- 3532** Hepatitis B core-related antigen: Are we near a treatment endpoint?

Gupta T

ABOUT COVER

Editorial Board Member of *World Journal of Gastroenterology*, Govind K Makharia, MD, DM, DNB, Professor, Department of Gastroenterology and Human Nutrition, All India Institute of Medical Sciences, Ansari Nagar, New Delhi 110029, India. govindmakharia@aiims.edu

AIMS AND SCOPE

The primary aim of *World Journal of Gastroenterology* (WJG, *World J Gastroenterol*) is to provide scholars and readers from various fields of gastroenterology and hepatology with a platform to publish high-quality basic and clinical research articles and communicate their research findings online. WJG mainly publishes articles reporting research results and findings obtained in the field of gastroenterology and hepatology and covering a wide range of topics including gastroenterology, hepatology, gastrointestinal endoscopy, gastrointestinal surgery, gastrointestinal oncology, and pediatric gastroenterology.

INDEXING/ABSTRACTING

The WJG is now abstracted and indexed in Science Citation Index Expanded (SCIE, also known as SciSearch®), Current Contents/Clinical Medicine, Journal Citation Reports, Index Medicus, MEDLINE, PubMed, PubMed Central, Scopus, Reference Citation Analysis, China National Knowledge Infrastructure, China Science and Technology Journal Database, and Superstar Journals Database. The 2022 edition of Journal Citation Reports® cites the 2021 impact factor (IF) for WJG as 5.374; IF without journal self cites: 5.187; 5-year IF: 5.715; Journal Citation Indicator: 0.84; Ranking: 31 among 93 journals in gastroenterology and hepatology; and Quartile category: Q2. The WJG's CiteScore for 2021 is 8.1 and Scopus CiteScore rank 2021: Gastroenterology is 18/149.

RESPONSIBLE EDITORS FOR THIS ISSUE

Production Editor: Wen-Wen Qi; Production Department Director: Xiang Li; Editorial Office Director: Jia-Ru Fan.

NAME OF JOURNAL

World Journal of Gastroenterology

ISSN

ISSN 1007-9327 (print) ISSN 2219-2840 (online)

LAUNCH DATE

October 1, 1995

FREQUENCY

Weekly

EDITORS-IN-CHIEF

Andrzej S Tarnawski

EDITORIAL BOARD MEMBERS

<http://www.wjgnet.com/1007-9327/editorialboard.htm>

PUBLICATION DATE

July 21, 2022

COPYRIGHT

© 2022 Baishideng Publishing Group Inc

INSTRUCTIONS TO AUTHORS

<https://www.wjgnet.com/bpg/gerinfo/204>

GUIDELINES FOR ETHICS DOCUMENTS

<https://www.wjgnet.com/bpg/GerInfo/287>

GUIDELINES FOR NON-NATIVE SPEAKERS OF ENGLISH

<https://www.wjgnet.com/bpg/gerinfo/240>

PUBLICATION ETHICS

<https://www.wjgnet.com/bpg/GerInfo/288>

PUBLICATION MISCONDUCT

<https://www.wjgnet.com/bpg/gerinfo/208>

ARTICLE PROCESSING CHARGE

<https://www.wjgnet.com/bpg/gerinfo/242>

STEPS FOR SUBMITTING MANUSCRIPTS

<https://www.wjgnet.com/bpg/GerInfo/239>

ONLINE SUBMISSION

<https://www.f6publishing.com>



Basic Study

Accumulation of poly (adenosine diphosphate-ribose) by sustained supply of calcium inducing mitochondrial stress in pancreatic cancer cells

Keun-Yeong Jeong, Jae Jun Sim, Minhee Park, Hwan Mook Kim

Specialty type: Gastroenterology and hepatology

Provenance and peer review: Invited article; Externally peer reviewed.

Peer-review model: Single blind

Peer-review report's scientific quality classification

Grade A (Excellent): 0
Grade B (Very good): B
Grade C (Good): C, C
Grade D (Fair): 0
Grade E (Poor): 0

P-Reviewer: Prasetyo EP, Indonesia; Tang D, China; Zuo CJ, China

Received: January 11, 2022

Peer-review started: January 11, 2022

First decision: March 8, 2022

Revised: March 15, 2022

Accepted: June 26, 2022

Article in press: June 26, 2022

Published online: July 21, 2022



Keun-Yeong Jeong, Jae Jun Sim, Minhee Park, Hwan Mook Kim, Research and Development, Metimedi Pharmaceuticals, Incheon 22006, South Korea

Corresponding author: Keun-Yeong Jeong, PhD, Executive Vice President, Research Assistant Professor, Research and Development, Metimedi Pharmaceuticals, 263 Central-ro, Incheon 22006, South Korea. alvirus@naver.com

Abstract

BACKGROUND

The biochemical phenomenon defined as poly adenosine diphosphate (ADP)-ribosylation (PARylation) is essential for the progression of pancreatic cancer. However, the excessive accumulation of poly ADP-ribose (PAR) induces apoptosis-inducing factor (AIF) release from mitochondria and energy deprivation resulting in the caspase-independent death of cancer cells.

AIM

To investigate whether sustained calcium supply could induce an anticancer effect on pancreatic cancer by PAR accumulation.

METHODS

Two pancreatic cancer cell lines, AsPC-1 and CFPAC-1 were used for the study. Calcium influx and mitochondrial reactive oxygen species (ROS) were observed by fluorescence staining. Changes in enzyme levels, as well as PAR accumulation and energy metabolism, were measured using assay kits. AIF-dependent cell death was investigated followed by confirming *in vivo* anticancer effects by sustained calcium administration.

RESULTS

Mitochondrial ROS levels were elevated with increasing calcium influx into pancreatic cancer cells. Then, excess PAR accumulation, decreased PAR glycohydrolase and ADP-ribosyl hydrolase 3 levels, and energy deprivation were observed. *In vitro* and *in vivo* antitumor effects were confirmed to accompany elevated AIF levels.

CONCLUSION

This study visualized the potential anticancer effects of excessive PAR accumu-

lation by sustained calcium supply on pancreatic cancer, however elucidating a clear mode of action remains a challenge, and it should be accompanied by further studies to assess its potential for clinical application.

Key Words: Pancreatic cancer; Calcium; Reactive oxygen species; Poly adenosine diphosphate-ribose; Poly adenosine diphosphate-ribosylation; Poly adenosine diphosphate-ribose polymerase; Apoptosis-inducing factor; Nicotinamide adenine dinucleotide; Anticancer effect

©The Author(s) 2022. Published by Baishideng Publishing Group Inc. All rights reserved.

Core Tip: Accumulation of poly adenosine diphosphate-ribose (PAR) was induced by an increase in reactive oxygen species following sustained calcium supply, which in turn led to the death of pancreatic cancer cells by energy deprivation and apoptosis-inducing factor expression. Although calcium-mediated accumulation of PAR would be a potential strategy for the treatment of pancreatic cancer, the association with the mechanical role of calcium in enabling the inactivation of PAR-degrading enzymes needs to be elucidated.

Citation: Jeong KY, Sim JJ, Park M, Kim HM. Accumulation of poly (adenosine diphosphate-ribose) by sustained supply of calcium inducing mitochondrial stress in pancreatic cancer cells. *World J Gastroenterol* 2022; 28(27): 3422-3434

URL: <https://www.wjgnet.com/1007-9327/full/v28/i27/3422.htm>

DOI: <https://dx.doi.org/10.3748/wjg.v28.i27.3422>

INTRODUCTION

Recent literature emphasizes that the biochemical phenomenon defined as poly adenosine diphosphate (ADP)-ribosylation (PARylation) is essential for the progression of cancer[1]. Poly ADP-ribose (PAR) is synthesized by the biochemical reaction of PAR polymerase-1 (PARP-1), which catalyzes the polymerization of ADP-ribose from the donor nicotinamide adenine dinucleotide (NAD⁺) to form a linear or branched PAR polymer[2]. Because PARylation is implicated in the multistep process involving various physiological maintenance factors and overcoming stress conditions for cancer cell survival, there might be connections between PARP-1 function and pancreatic cancer progression as a bridgehead linked by PARylation[1,2].

Although PARylation is essential for cancer survival, the excessive accumulation of PAR can mediate apoptosis-inducing factor (AIF) release from mitochondria and its nuclear translocation, resulting in the caspase-independent death of cancer cells[3]. The mode of action of the relationship between AIF and PAR involved in cell death has not been elucidated, but AIF translocation to the nucleus leading to chromatin condensation and large-scale DNA fragmentation is a well-established theory[3,4]. Cell death following PAR accumulation was recently defined as parthanatos, which is considered another death mechanism in a large category of apoptosis-type reactions[4]. Therefore, targeting ADP-ribosyl hydrolase 3 (ARH3), a type of PAR-degrading protein, and PAR glycohydrolase (PARG), a reversible covalent-modifier targeting PAR, might be potential methods to induce anticancer effects *via* PAR accumulation[5-7]. Although approaches to inhibit such enzymes through RNA interference or genetic manipulation have been tried, there have been few studies of the relevant mechanisms targeting pancreatic cancer[6,7].

Calcium is a key element in physiological signal transduction that enables the adjustment of energy production to cellular demand[8]; however, some reports indicated that cancer cells were affected during the influx of a high concentration of calcium resulting in excessive reactive oxygen species (ROS) produced from mitochondria[9]. Furthermore, there was an association between PARP-1 and an increase in ROS[1,10,11]. It was reported that the hyperactivation of PARP-1 was induced by an increase in ROS caused by intracellular calcium influx, the activation of PARP-1 as a response to DNA damage, or to drive an antioxidant program to protect cells from ROS[1,10,11]. This implies that excessive PAR accumulation can be induced as a result of PARP-1 hyperactivation followed by PARylation, suggesting the prospect of influencing pancreatic cancer cell survival by supplying high concentrations of calcium. The study aimed to investigate whether a sustained calcium supply induced intracellular PAR accumulation with an increase in ROS and to demonstrate the potential of this phenomenon to promote anticancer effects on pancreatic cancer.

MATERIALS AND METHODS

Cell lines and culture conditions

AsPC-1 and CFPAC-1 were obtained from the American Type Culture Collection (Manassas, VA, United States). The cells were grown in Roswell Park Memorial Institute 1640 and Iscove's Modified Dubecco's Medium supplemented with 10% fetal bovine serum (Welgene, Gyeongsan, Korea) and 1% penicillin/streptomycin (Welgene, Gyeongsan, Korea). All cells were cultured under a humidified atmosphere at 37 °C containing 5% CO₂.

Reagents

Lactate calcium salt (CaLac) and calpeptin were purchased from Sigma-Aldrich (St. Louis, MO, United States) and dissolved in distilled water. The solutions were stored at 4 °C until use.

Measurement of intracellular calcium

Calcium concentrations were measured using a confocal laser scanning microscope (Leica, Heidelberg, Germany). Cultured pancreatic cancer cells were loaded with 10 μM Fluo-3/AM (Invitrogen, Frederick, MD, United States) dissolved in dimethyl sulfoxide (Sigma-Aldrich). Then the cells were incubated for 30 min at 37 °C. Fluo-3/AM was excited at 488 nm and emitted fluorescence was measured at 515 nm.

Immunocytochemistry

Pancreatic cancer cells were fixed on bio-coated coverslips (BD bioscience, NJ, United States) using 4% paraformaldehyde, and incubated for 15 h with the primary antibody against AIF (1:200, Santa Cruz Biotechnology, Santa Cruz, CA, United States). Subsequently, the cells were incubated with an anti-rabbit secondary biotinylated anti-body (1:5000, Abcam) and visualized with streptavidin conjugated to fluorescein (Vector Laboratories, Burlingame, CA, United States). MitoSOX Red (Thermo Fisher Scientific, Waltham, MA, United States) was used to detect mitochondrial superoxide production. Fluorescence was measured using a confocal laser scanning microscope (Leica). Signal intensities were quantified and analyzed using the Xenogen Imaging System (IVIS® 100 series, Caliper Life Science, MA, United States).

Enzyme-linked immunosorbent assay

PARG, RNF-146, PAR, and AIF levels were quantified from 1 × 10⁶ number of pancreatic cancer cells or 2 mm³ volume of tumor tissues using each assay kit (PARG assay kit: Trevigen, Gaithersburg, MD, United States; RNF-146 ELISA kit: Abbexa, Houston, TX, United States; PAR ELISA kit: Cell Biolabs, San Diego, CA, United States; AIF ELISA kit: Abcam, Cambridge, England), according to the manufacturer's instructions.

Adenosine triphosphate assay

The cell culture medium was supplemented with CaLac, and cultures were incubated for 24 h. 1 × 10⁶ cells were then sonicated. The cells were centrifuged at 1500 g for 20 min to remove insoluble material, and the supernatant was collected. Adenosine triphosphate (ATP) was measured by ATP colorimetric assay kit (Abcam) according to manufacturer's instructions.

NAD⁺ and NADH assay

The cell culture medium was supplemented with CaLac, and the cultures were incubated for 24 h. 1 × 10⁶ cells were then sonicated. The cells were washed twice with phosphate buffer solution (PBS), and NAD⁺ and NADH levels were measured using the NAD/NADH quantitation kit (Sigma) according to the manufacturer's protocol.

Transferase-mediated dUTP nick end labeling assay

Pancreatic cancer cells were treated with CaLac for 24 h and then washed with cold PBS. The cells were fixed with 4% paraformaldehyde for 30 min and washed twice with PBS for 2 min. Fixed cells in permeabilization solution (0.1% Triton X-100 and 0.1% Sodium citrate) were washed. The tumors were fixed in 10% neutral buffered formalin and embedded in paraffin. Tissue sections (4 μm) were made from paraffin-embedded blocks on a microtome, and then the sections were deparaffinized and rehydrated. To detect cell death, the DeadEnd™ Fluorometric transferase-mediated dUTP nick end labeling (TUNEL) system kit (Promega, Madison, WI, United States) was used according to the manufacturer's instructions.

FACS analysis

Annexin V and propidium iodide (PI) staining was performed using an Annexin V-FITC Apoptosis Detection Kit (BD Biosciences). 2.5 × 10⁶ of AsPC-1 and CFPAC-1 cells were exposed to CaLac for 24 h. The cells were resuspended in 100 μL of Annexin V-FITC binding buffer, and then 5 μL of Annexin V-FITC conjugate and 10 μL of PI buffer were added. Annexin V and PI were analyzed using a FACS

Calibur™ instrument (BD Biosciences).

Cell viability assay

Pancreatic cancer cells were cultured in a 96-well plate (3×10^3 cells/well) for 24 h, and then treated with CaLac for 24 h at 37 °C. Then, 10 μ L of 3-(4,5-dimethylthiazol-2-yl)-2,5-diphenyltetrazolium bromide was added to each well, and the cells were incubated at 37 °C for 1 h in a humidified environment containing 5% CO₂. After the media was discarded, 200 μ L of dimethyl sulfoxide (Cell Signaling Technology, Danvers, MA, United States) was added to each well. The absorbance was read at 570 nm using a microplate reader (iMark Microplate Absorbance Reader, Bio-Rad, CA, United States).

Xenograft animal model

Twenty-eight male Balb/c nude mice (5 wk of age) were purchased from the Charles River Breeding Laboratories (Wilmington, MA, United States). All animals were maintained on a 12 h light/dark cycle (light on, 08:00) at 22–25 °C, with free access to food and water. To investigate the antitumor activity of CaLac *in vivo*, a therapeutic strategy was devised to investigate its effect on the heterotopic xenograft animal model. Fourteen mice were used for establishing a heterotopic xenograft model using AsPC-1 cells (5×10^6) resuspended in 100 μ L of phosphate-buffered saline. The cells were injected subcutaneously into the left flank of mice. Once the tumors reached a diameter of 8 mm, 7 mice were randomly divided into the untreated group, and 7 mice were divided into the CaLac-treated group. 20 mg/kg of CaLac was subcutaneously injected daily for 21 d. Tumor growth was monitored three times per week. To harvest tumors for histological and molecular biology analysis, carbon dioxide inhalation was used for euthanasia at the end of the experiments.

Immunohistochemistry

The tumors were fixed in 10% neutral buffered formalin and embedded in paraffin. Tissue sections (4 μ m) were made from paraffin-embedded blocks on a microtome, and then the sections were deparaffinized and rehydrated. Endogenous peroxidase activity was blocked by 3% H₂O₂ in distilled water for 30 min. Antigen retrieval was induced by slide heating with 10 mmol/L citrate buffer (pH 6.0) using a microwave oven. The sections were blocked using a blocking agent (Invitrogen, Frederick, MD, United States) and incubated overnight with the primary antibodies at 4 °C. The primary antibodies were as follows: Ki-67 (1:200, Santa Cruz Biotechnology) and proliferating cell nuclear antigen (PCNA, 1:200, Santa Cruz Biotechnology). The sections were then incubated with biotinylated anti-mouse antibody (1:500, Vector Laboratories, Burlingame, CA, United States) for 1 h. After a PBST wash, the sections were treated with 3,3'-diaminobenzidine substrate (Dako, Carpinteria, CA, United States) and counterstained with hematoxylin (Thermo Fisher Scientific). A Leica DM 1000 LED microscope (Leica Microsystems, Wetzlar, Germany) was used for image analysis.

Statistical analysis

Data are presented as the means \pm SD. Statistical significance was analyzed using the Student's *t*-test or one-way analysis of variance, depending on the normality of the data distribution. *P* < 0.05 was considered as statistically significant. All statistical analyses were performed by Sigma Stat v3.5 (Systat Software Inc., Chicago, IL, United States).

RESULTS

Calcium influx increases mitochondrial ROS in pancreatic cancer cells

The fluorescence intensity of fluo-3 by calcium reaction was increased in cells of both types of pancreatic cancer, AsPC-1 and CFPAC-1, following CaLac treatment (Figure 1A). In a quantitative analysis of fluorescence intensity, intracellular calcium levels were significantly increased by sustained calcium supply to about 2.1- and 1.9-fold in AsPC-1 and CFPAC-1, respectively, compared with the untreated group (Figure 1B). The increase in red fluorescence level in pancreatic cancer cells indicated increased ROS generation in pancreatic cancer cells by sustained calcium supply, indicating that ROS originated from mitochondria by the simultaneous use of a mitochondrial tracer showing green fluorescence (Figure 1C). In an analysis of the mean fluorescence intensity (MFI), mitochondrial ROS levels detected by MitoSOX™ were significantly increased by sustained calcium supply to about 2.33- and 2.63-fold in AsPC-1 and CFPAC-1, respectively, compared with the untreated group (Figures 1D and E).

An increase in ROS causes the excessive accumulation of PAR and energy deprivation

In addition to the immediate association of PAR accumulation by increased ROS levels, PARG and RNF-146 were supplementally investigated to confirm a change in the enzyme levels involved in PAR accumulation. A decrease in the enzymatic activity of PARG and ARH3 following calcium supply was observed (Figures 2A and B), accompanied by the accumulation of PAR in pancreatic cancer cells (Figure 2C). Changes in coenzyme factors involved in energy metabolism following the accumulation of

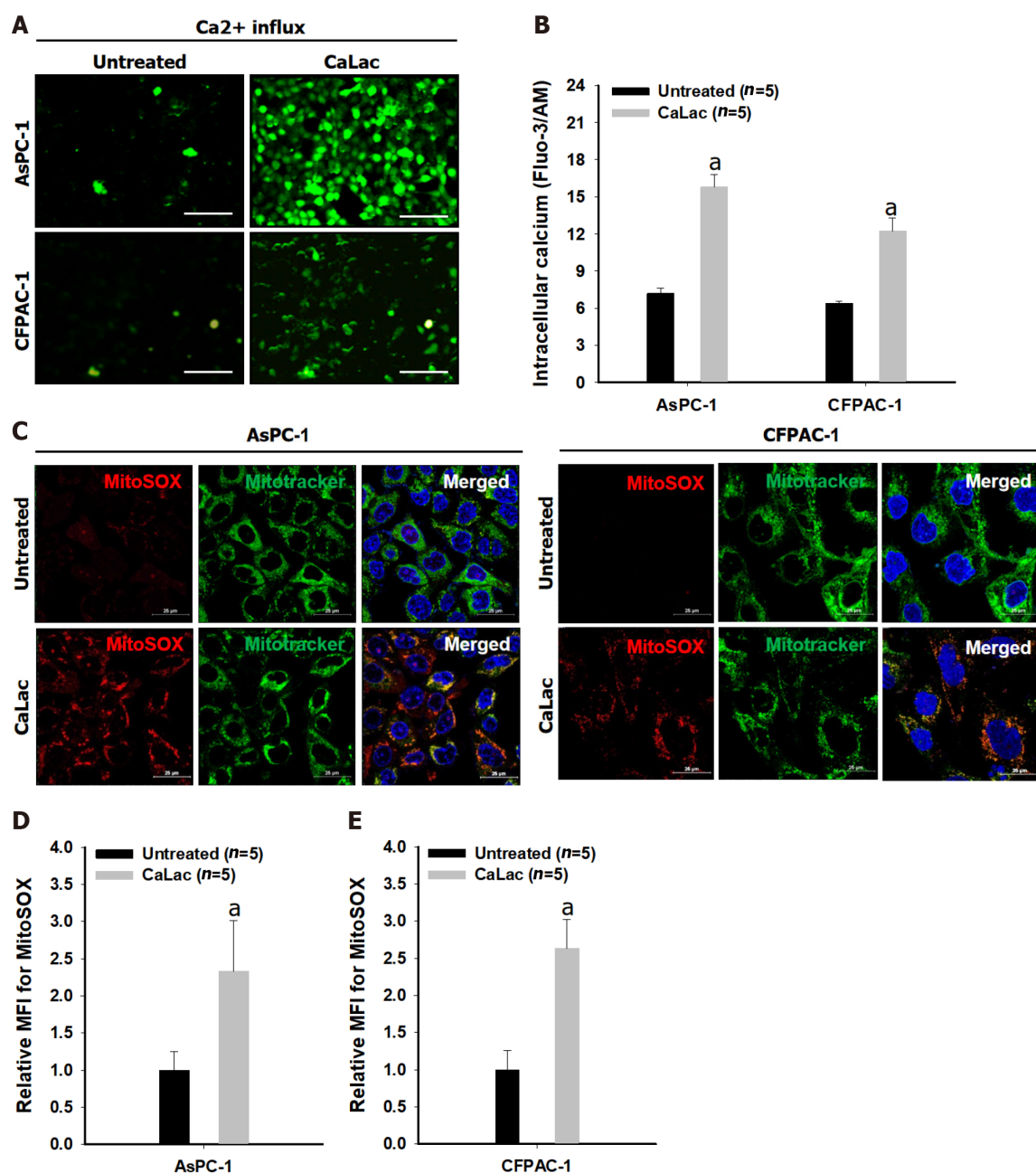


Figure 1 Confirmation of mitochondrial reactive oxygen species generation by sustained calcium supply. A: Fluorescent calcium imaging following lactate calcium salt (CaLac) treatment of pancreatic cancer cells (AsPC-1 and CFPAC-1). Scale bars: 100 μ m; B: Quantitative analysis of the fluorescence intensity of calcium; C: Confocal imaging of mitochondrial reactive oxygen species (ROS) in pancreatic cancer cells. Red dye: Mitochondrial superoxide indicator; Green dye: Mitochondrial indicator. Scale bars: 25 μ m; D: Quantitative analysis of the fluorescence intensity of mitochondrial ROS in AsPC-1; E: Quantitative analysis of the fluorescence intensity of mitochondrial ROS in CFPAC-1. The fluorescence intensity was calculated by the mean fluorescence intensity. The cells were treated with 2.5 mM CaLac for 72 h. Results represent the mean \pm SD. ^a $P < 0.001$ vs untreated. CaLac: Lactate calcium salt; MitoSOX: Mitochondrial superoxide indicator.

PAR were also identified (Figures 2D and E). These results indicated that the excessive synthesis of PAR resulted in reduced NAD⁺ levels (Figure 2D) and the increase of NADH levels (Figure 2E), which led to a depletion of ATP (Figure 2F).

An increase in AIF expression induces the death of pancreatic cancer cells

The results of immunocytochemical staining for the co-expression of AIF with the mitochondrial tracker in two types of pancreatic cancer cells indicated the calcium supply induced the translocation of AIF from the cytoplasm into the nucleus, whereas only cytoplasmic co-expression was observed in the untreated group (Figure 3A). Furthermore, it was quantitatively increased by calcium supply when the expression of AIF only was confirmed as a separate result through MFI analysis (Figures 3B and C). Then, the reaction ratio by TUNEL staining per total cells was significantly increased (Figures 3D and E), and Annexin V labeled cells increased from 6.61% to 37.61% and from 4.8% to 26.91% in AsPC-1 and CFPAC-1, respectively (Figure 3F). A decrease in cell viability by calcium supply was macroscopically

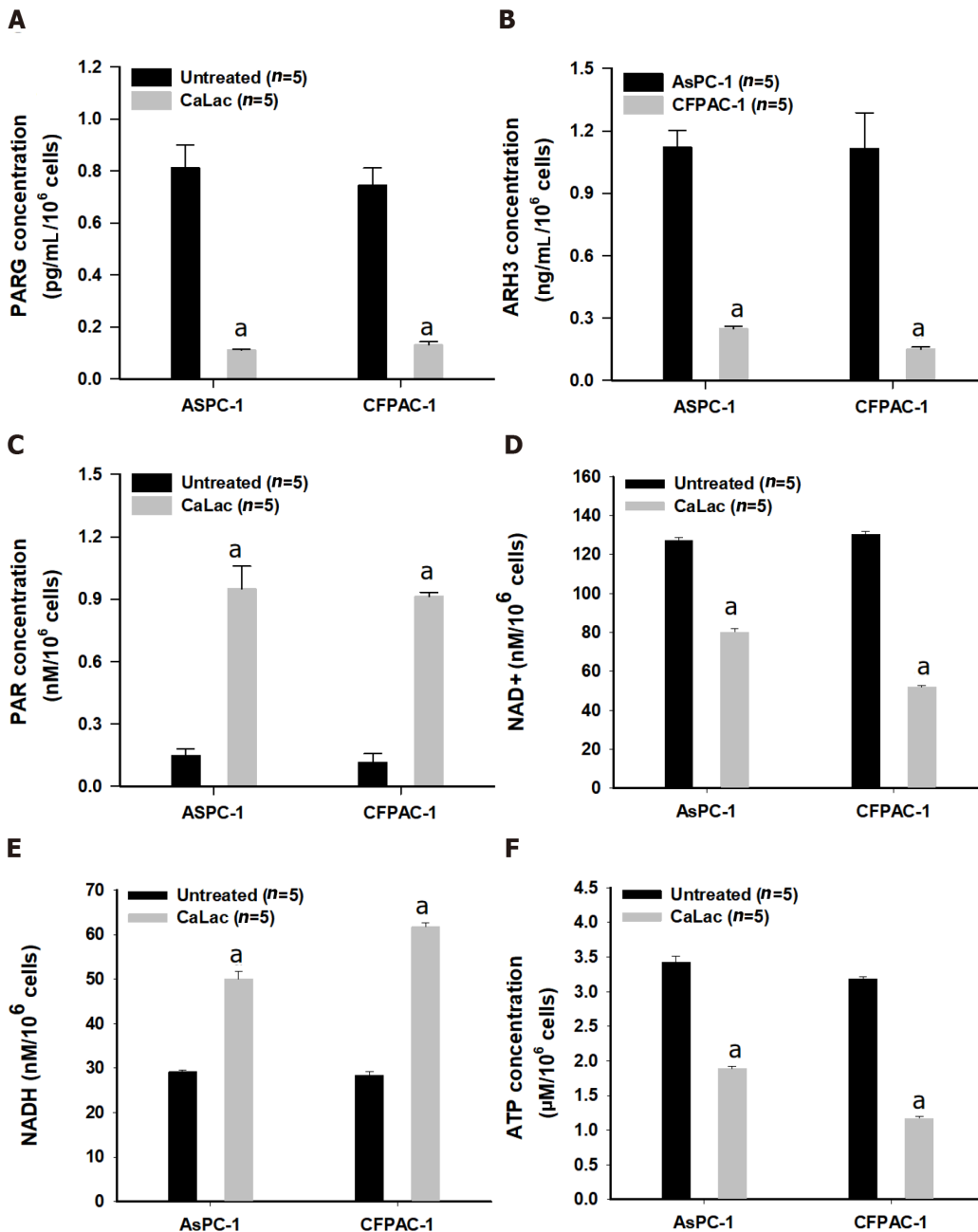


Figure 2 Confirmation of enzyme change and poly adenosine diphosphate-ribose accumulation by calcium supply resulting in energy crisis. A: Quantitative analysis of the enzyme levels of poly adenosine diphosphate (ADP)-ribose (PAR) glycohydrolase in pancreatic cancer cells (AsPC-1 and CFPAC-1); B: Quantitative analysis of the enzyme levels of ADP-ribosyl hydrolase 3 in AsPC-1 and CFPAC-1; C: Quantitative analysis of PAR levels; D: Quantitative analysis of nicotinamide adenine dinucleotide levels; E: Quantitative analysis of NADH levels; F: Quantitative analysis of adenosine triphosphate (ATP) levels. The cells were treated with 2.5 mM lactate calcium salt for 72 h. Results represent the mean \pm SD. ^a $P < 0.001$ vs untreated. CaLac: Lactate calcium salt; PARG: Poly adenosine diphosphate-ribose glycohydrolase; ARH3: Adenosine diphosphate-ribosyl hydrolase 3; NAD⁺: Nicotinamide adenine dinucleotide; ATP: Adenosine triphosphate.

observed by microphotographs (Figure 3G), and the CaLac group (calcium supply) showed low cell viability (mean 35.5%) when defining the total cell viability of the untreated group as 100% (Figure 3H).

An increase in PAR accumulation relates to calcium-dependent proteolytic enzyme activity in pancreatic cancer cells

To elucidate an increase in PAR accumulation by sustained calcium supply, the calpain inhibitor, calpeptin, was introduced. Changes in PARG, ARH3, PAR, and AIF were sequentially observed in pancreatic cancer cells (Figure 4). Although PARG levels were significantly decreased by sustained calcium supply, there was only a slight decrease (no significant difference) when combining calpeptin with calcium supply (Figures 4A and B). Calpeptin itself did not directly change the levels of PARG (Figures 4A and B) similar to that of ARH3 (Figures 4C and D). Furthermore, the levels of PAR and AIF

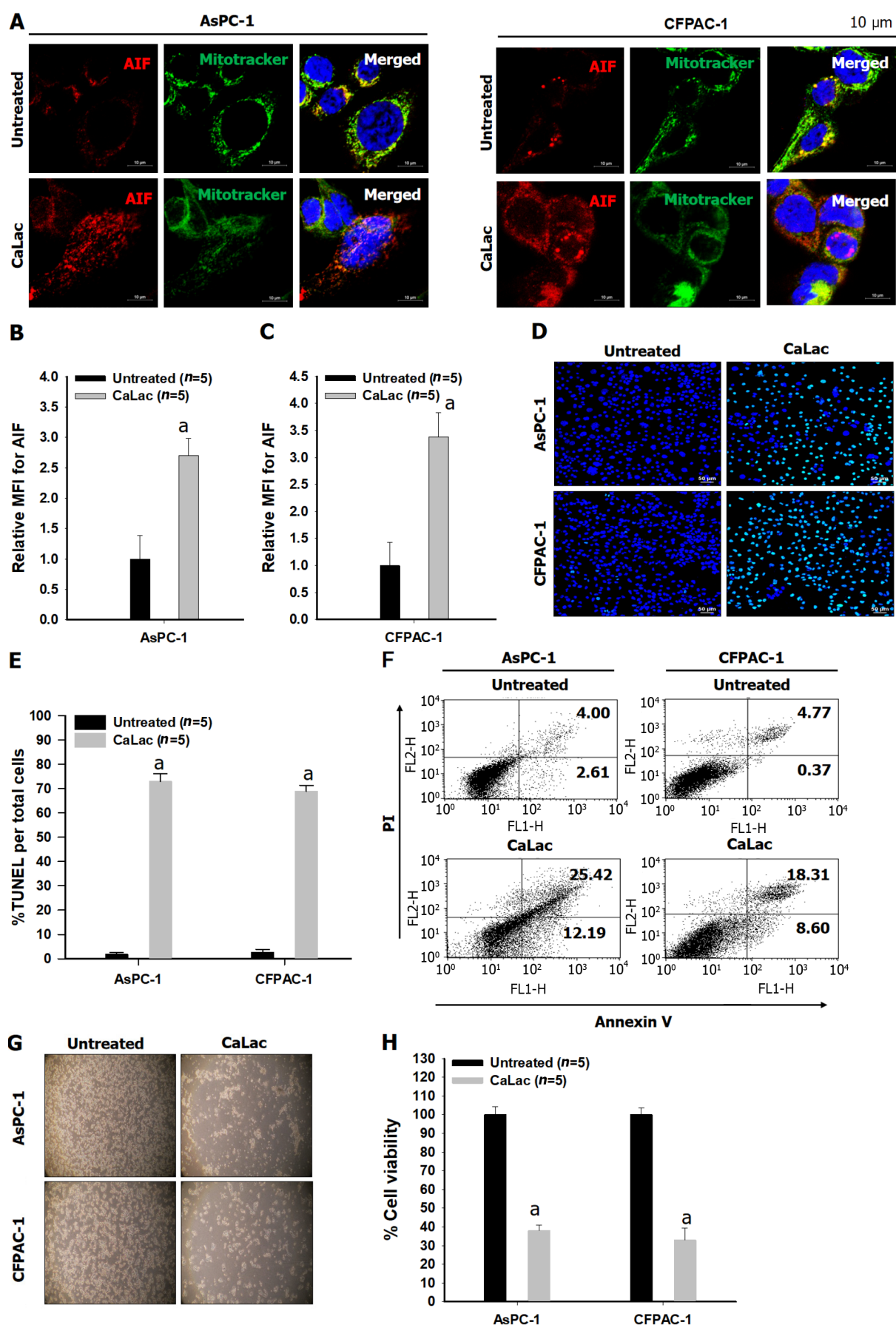


Figure 3 Confirmation of the expression of apoptosis-inducing factor followed by an increase in apoptosis in pancreatic cancer cells (AsPC-1 and CFPAC-1). A: Immunocytochemical staining for apoptosis-inducing factor (AIF) release from mitochondria and translocation into the nucleus. Red dye: AIF; Green dye: Mitochondrial indicator. Scale bars: 10 μ m; B: Quantitative analysis of the mean fluorescence intensity (MFI) of AIF in CFPAC-1; C: Quantitative

analysis of the MFI of AIF in AsPC-1; D: Fluorescent microphotographs for colorimetric terminal deoxynucleotidyl transferase -mediated dUTP nick end labeling (TUNEL) detection. Green dye: TUNEL staining. Scale bars: 50 μ m; E: Quantitative analysis of the % ratio of TUNEL detected cells per total pancreatic cancer cells; F: Representative flow cytometry plots using Annexin V-fluorescein-5-isothiocyanate/propidium iodide staining for apoptosis; G: Representative microphotographs to compare cell condition after calcium supply; H: Quantitative analysis of the percent cell viability following calcium supply. The cells were treated with 2.5 mM lactate calcium salt for 72 h. Results represent the mean \pm SD. ^a P < 0.001 vs untreated. CaLac: Lactate calcium salt; AIF: Apoptosis-inducing factor; MFI: Mean fluorescence intensity; TUNEL: Transferase-mediated dUTP nick end labeling.

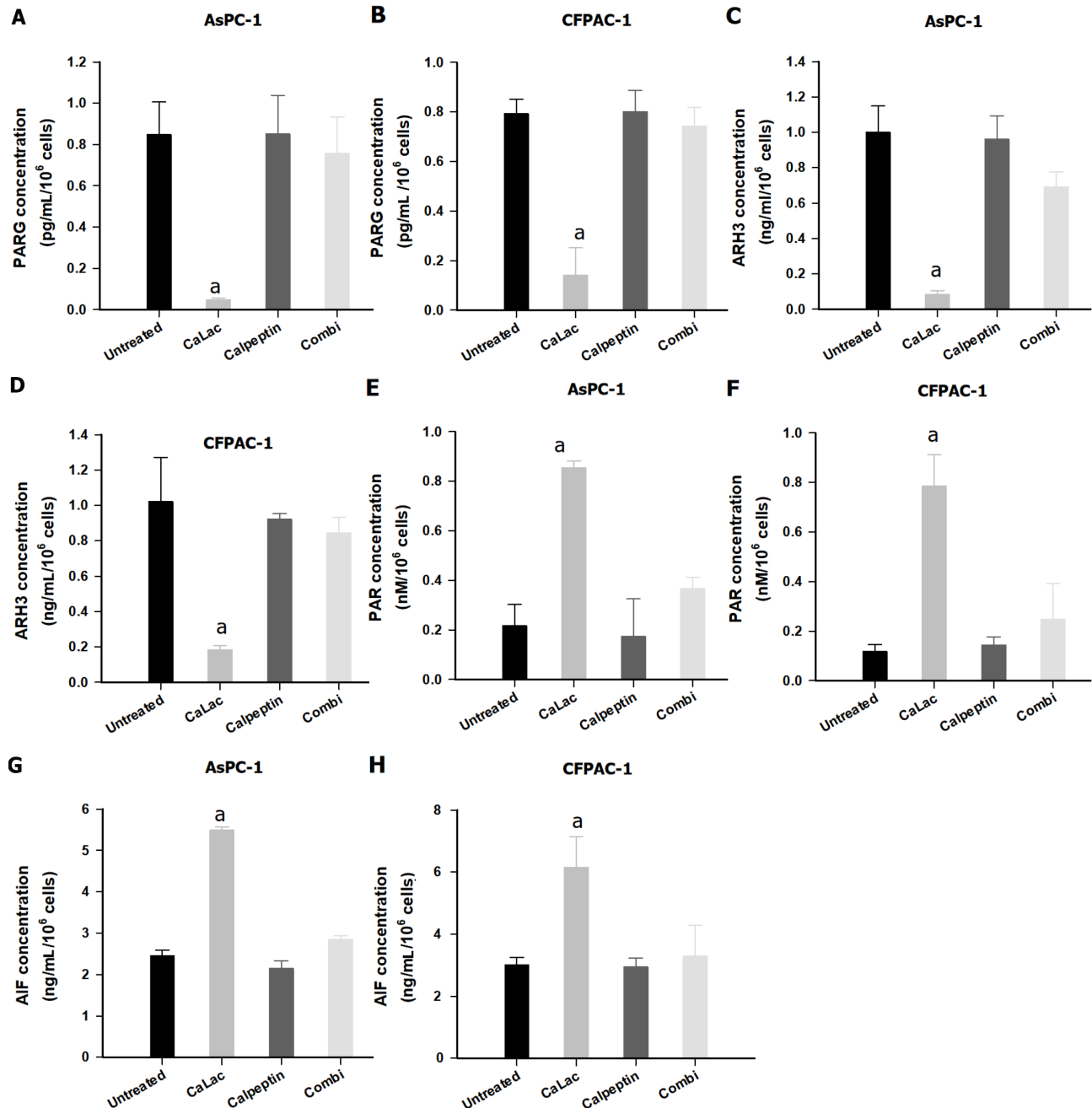


Figure 4 Confirmation of poly-adenosine diphosphate ribose accumulation in pancreatic cancer cells (AsPC-1 and CFPAC-1) by calcium-mediated proteasomal activity. A: Quantitative analysis of poly adenosine diphosphate-ribose glycohydrolase (PARG) levels in AsPC-1; B: Quantitative analysis of PARG levels in CFPAC-1; C: Quantitative analysis of ADP-ribosyl hydrolase 3 (ARH3) levels in AsPC-1; D: Quantitative analysis of ARH3 levels in CFPAC-1; E: Quantitative analysis of PAR levels in AsPC-1; F: Quantitative analysis of PAR levels in CFPAC-1; G: Quantitative analysis of apoptosis-inducing factor (AIF) levels in AsPC-1; H: Quantitative analysis of AIF levels in CFPAC-1. Calpeptin was used for proteasome inhibition. The cells were treated with 2.5 mM lactate calcium salt for 72 h. Results represent the mean \pm SD. ^a P < 0.001 vs untreated. CaLac: Lactate calcium salt; PARG: Poly adenosine diphosphate-ribose glycohydrolase; ARH3: Adenosine diphosphate-ribosyl hydrolase 3; AIF: Apoptosis-inducing factor.

were increased by calcium supply, which was restored to a level similar to that of the untreated group under culture conditions in which calpeptin was added (Figures 4E-H).

Sustained calcium administration induces anticancer effects on pancreatic cancer

Comparative results of tumor growth in heterotopic xenograft models demonstrated the inhibition of pancreatic cancer growth by calcium administration (Figures 5A and B, Figure 6). The tumor volume on the last day of measurement was 830.37 ± 138.36 and 431.41 ± 91.98 in the untreated and the CaLac groups, respectively. Tumor volume was reduced by about 48.1% in the CaLac group compared with the untreated group (Figure 5B). There were few viable cells capable of discriminating the staining of nuclei in tumor tissues of the CaLac group (Figure 5C), indicating an increase in PAR-dependent AIF expression following sustained calcium-induced apoptosis (Figures 5D and E). The apoptotic signal in tumor tissues was increased 5.13-fold in the CaLac group compared with the untreated group (Figures 5F and G). As a result of apoptosis, the malignancy indicators of tumors were significantly reduced (Figure 5H) and the expressions of Ki-67 and PCNA were significantly reduced by about 64% and 68%, respectively in the CaLac group (Figures 5I and J).

DISCUSSION

This study demonstrated that the accumulation of PAR was induced by an increase in ROS following sustained calcium supply, which in turn led to the death of pancreatic cancer cells by energy deprivation and AIF expression. CaLac is a small molecule generated by the reaction of lactic acid with calcium carbonate and is characterized as a weak electrolyte with a neutralized charge[12]. Such a characteristic of CaLac suggests it might readily cross cell membranes as a bound form. Therefore, the accumulation of calcium was greatly increased in pancreatic cancer cells by the sustained treatment of CaLac, which was in line with our direction of research targeting intracellular calcium accumulation. It is well known that intracellular calcium uptake can promote ROS formation in mitochondria by stimulating tricarboxylic acid cycle enzymes and electron transport chain activity[9]. The results indicated that calcium accumulation by CaLac led to an increase in the mitochondrial ROS of pancreatic cancer cells. An active calcium signal must operate within physiological levels, but when intracellular calcium levels exceed this threshold, excessive ROS production can have a detrimental effect on cell survival by disrupting mitochondrial bioenergetic regulation and cellular functions[13]. The main reason for investigating an increase in PAR synthesis among the various biological phenomena mediated by calcium-dependent excessive ROS is its key function as a protective mechanism for cancer cell survival under hostile conditions[1,10,11,14]. ROS can be spontaneously generated during the ceaseless process of the rapid growth of cancer cells, but excessive ROS can cause DNA damage by irreversible oxidative stress[15]. PAR synthesis is defined as PARylation by PARP-1 recruits or modifies several nuclear proteins during the DNA damage response against harmful oxidative stress; however, the excessive synthesis of PAR can lead to cell death[1,14]. A sustained calcium supply causes the accumulation of PAR to cope with long-lasting DNA damage along with an increase of ROS in pancreatic cancer cells. Well-established phenomena induced by PAR accumulation include energy deprivation and AIF release from mitochondria[3,4,16]. Because PAR is catalyzed for synthesis from donor NAD⁺, excessive PAR accumulation causes a decrease in the intracellular level of NAD⁺, leading to energy deprivation[8,17]. Furthermore, an increase in AIF release induces cell death by large-scale DNA fragmentation defined as parthanatos, although a clear mechanism has not been elucidated[4,16]. The results indicated that AIF migrates from the mitochondria to the cytoplasm and nucleus in response to the accumulation of PAR followed by inducing the death of pancreatic cancer cells. Therefore, excessive PAR accumulation caused by an increase in ROS by sustained calcium supply can be considered to mediate anticancer activity as the main mechanism with energy deprivation and AIF release in pancreatic cancer cells. Cancer cells activate PAR erasing enzymes PARG and ARH3 to hydrolyze ribose-ribose bonds, PAR itself, or O-acetyl-ADP-ribose resulting in the prevention of excessive PAR accumulation[6,18]. These hydrolytic reactions form a biochemical mechanism to counter the PAR-mediated death of cancer cells[4,19,20]. In this study, it was confirmed that the enzymatic activities of PARG and ARH3 were significantly decreased after sustained calcium supply; however, the activity was restored by treatment with calpeptin, a potent, cell-permeable calpain inhibitor. Calpain is a break-down molecule and a calcium-dependent cysteine protease that can also induce ROS production depending on its activation, and it may also damage ion channels, cell adhesion molecules, and cell surface receptors as well as various enzymes[21,22]. On this basis, it is anticipated that calcium-dependent calpain activation would directly induce the enzymatic inactivity of PARG and ARH according to the results of calpeptin application on pancreatic cancer cells. However, the current research outcome was unable to provide a clear mechanistic basis for the enzymatic inactivation of PARG and ARH by calpain. Because PARG and ARH3 are directly related to the accumulation of PAR in pancreatic cancer cells, we wish to investigate this further in more detail.

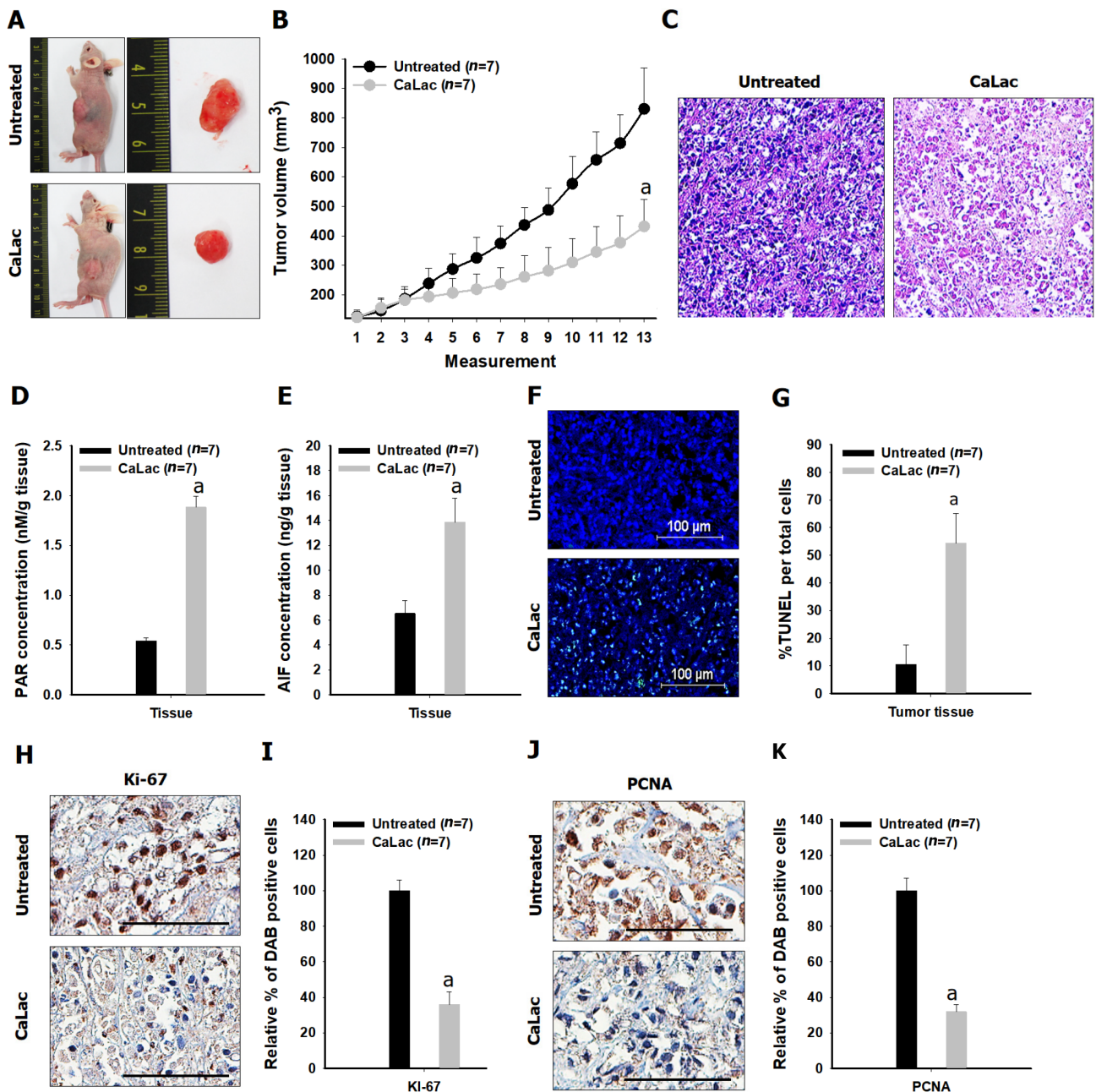


Figure 5 Confirmation of the *in vivo* antitumor effect on pancreatic cancer following sustained calcium administration. A: Macroscopic observation of the tumor mass; B: Comparison of tumor volume between the untreated and calcium-administered groups. Lactate calcium salt (CaLac): 20 mg/kg/mouse, subcutaneous injection, daily for 21 d; C: Hematoxylin and eosin staining. Scale bars: 100 μ m; D: Comparison of poly adenosine diphosphate ribose expression in tumor tissues; E: Comparison of apoptosis-inducing factor expression in tumor tissues; F and G: % terminal deoxynucleotidyl transferase-mediated dUTP nick end labeling expression to compare increased apoptosis in tumor tissues. Scale bars: 100 μ m; H and I: Comparison of Ki-67 expression in tumor tissues. Scale bars: 50 μ m; J and K: Comparison of proliferating cell nuclear antigen in tumor tissues. Scale bars: 50 μ m. ^a $P < 0.001$ vs untreated. Results are the mean \pm SD. PAR: Poly adenosine diphosphate ribose; AIF: Apoptosis-inducing factor; TUNEL: Transferase-mediated dUTP nick end labeling; PCNA: Proliferating cell nuclear antigen; CaLac: Lactate calcium salt.

CONCLUSION

This study focused on the accumulation of PAR to induce energy deprivation and AIF release by sustained calcium supply to investigate its potential anticancer effect on pancreatic cancer. We demonstrated that an increase in ROS and inhibition of PAR-erasing enzymes might be the main contributors to these effects. However, the connection to the mechanistic role of calcium in enabling the inactivation of PAR-degrading enzyme needs to be elucidated, and additional studies to explore the potential of clinical application are required.

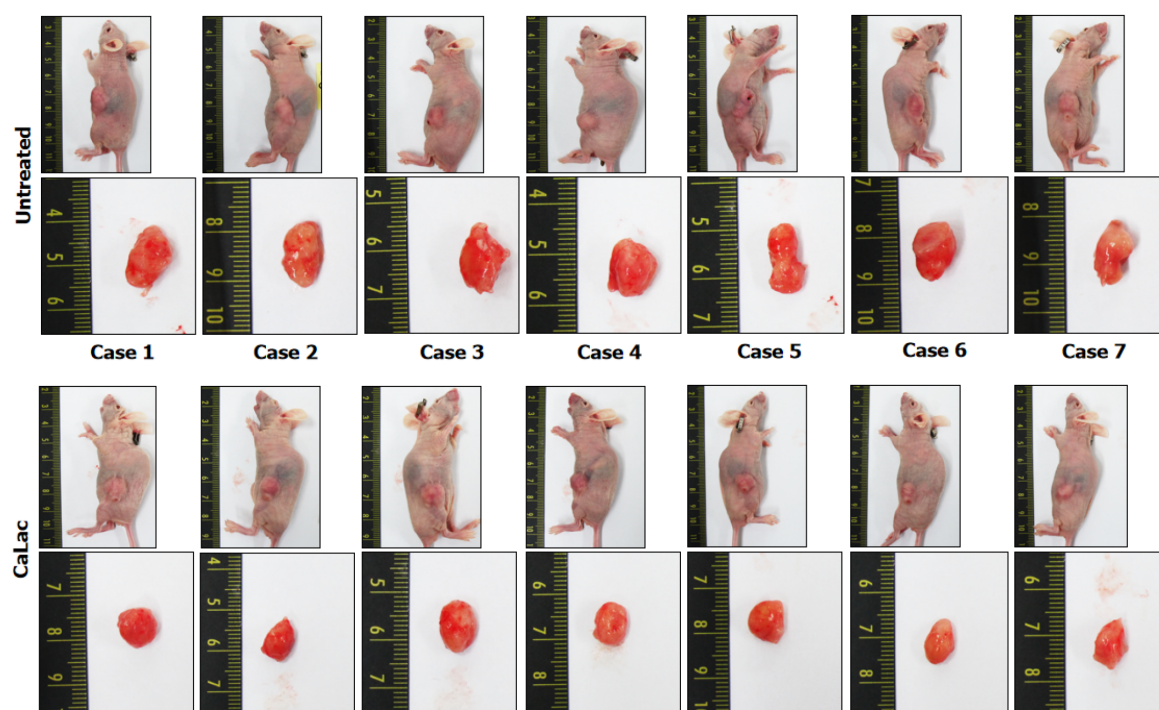


Figure 6 Tumor pictures of all xenograft mice following the end of 20 mg/kg lactate calcium salt administration for 21 d. CaLac: Lactate calcium salt.

ARTICLE HIGHLIGHTS

Research background

The excessive accumulation of poly adenosine diphosphate(ADP)-ribose (PAR) induces energy deprivation and apoptosis-inducing factor (AIF) release from mitochondria resulting in the caspase-independent death of cancer cells, and an increase in PAR is closely related to an increase in reactive oxygen species (ROS).

Research motivation

Increasing ROS can be induced in cancer cells by calcium influx. Therefore, it would be possible to expect the anticancer effect targeting pancreatic cancer through calcium-dependent PAR accumulation.

Research objectives

This study focused on the accumulation of PAR to induce energy deprivation and AIF release by sustained calcium supply to investigate its potential anticancer effect on pancreatic cancer.

Research methods

Two pancreatic cancer cell lines, AsPC-1 and CFPAC-1 were used for the study. Calcium influx and mitochondrial ROS were observed by fluorescence staining. Changes in enzyme levels, as well as PAR accumulation and energy metabolism, were measured using assay kits. AIF-dependent cell death was investigated followed by confirming *in vivo* anticancer effects by sustained calcium administration.

Research results

Mitochondrial ROS levels were elevated with increasing calcium influx into pancreatic cancer cells. Then, excess PAR accumulation, decreased PAR glycohydrolase and ADP-ribosyl hydrolase 3 levels, and energy crisis were observed. *In vitro* and *in vivo* antitumor effects were confirmed to accompany elevated AIF levels.

Research conclusions

Accumulation of PAR was induced by an increase in ROS following sustained calcium supply, which in turn led to the death of pancreatic cancer cells by energy deprivation and AIF expression. Calcium-mediated accumulation of PAR would be a potential strategy for the treatment of pancreatic cancer.

Research perspectives

Although this study visualized the potential anticancer effects of excessive PAR accumulation by sustained calcium supply on pancreatic cancer, elucidating a clear mode of action remains a challenge, and it should be accompanied by further studies to assess its potential for clinical application.

FOOTNOTES

Author contributions: Jeong KY conceived the project and wrote the paper; Jeong KY and Sim JJ designed the experiments; Jeong KY, Sim JJ, and Park MH performed the experiments; Jeong KY, Sim JJ, and Kim HM analyzed the data; and all authors discussed the results and revised the manuscript.

Institutional animal care and use committee statement: Animal care and experimental procedures were authorized by the Institutional Animal Care and Use Committee at Gachon University (IACUC-LCDI-2019-0102, 16 July 2019).

Conflict-of-interest statement: All the authors report no relevant conflicts of interest for this article.

Data sharing statement: No additional data are available.

ARRIVE guidelines statement: The authors have read the ARRIVE guidelines, and the manuscript was prepared and revised according to the ARRIVE guidelines.

Open-Access: This article is an open-access article that was selected by an in-house editor and fully peer-reviewed by external reviewers. It is distributed in accordance with the Creative Commons Attribution NonCommercial (CC BY-NC 4.0) license, which permits others to distribute, remix, adapt, build upon this work non-commercially, and license their derivative works on different terms, provided the original work is properly cited and the use is non-commercial. See: <https://creativecommons.org/licenses/by-nc/4.0/>

Country/Territory of origin: South Korea

ORCID number: Keun-Yeong Jeong 0000-0002-4933-3493; Jae Jun Sim 0000-0002-3851-5689; Minhee Park 0000-0002-2513-2080; Hwan Mook Kim 0000-0001-7649-9790.

S-Editor: Wang JJ

L-Editor: A

P-Editor: Qi WW

REFERENCES

- 1 Jeong KY, Park MH. The Significance of Targeting Poly (ADP-Ribose) Polymerase-1 in Pancreatic Cancer for Providing a New Therapeutic Paradigm. *Int J Mol Sci* 2021; **22** [PMID: 33805293 DOI: 10.3390/ijms22073509]
- 2 Alemasova EE, Lavrik OI. Poly(ADP-ribosylation) by PARP1: reaction mechanism and regulatory proteins. *Nucleic Acids Res* 2019; **47**: 3811-3827 [PMID: 30799503 DOI: 10.1093/nar/gkz120]
- 3 Kamaletdinova T, Fanaei-Kahrani Z, Wang ZQ. The Enigmatic Function of PARP1: From PARylation Activity to PAR Readers. *Cells* 2019; **8** [PMID: 31842403 DOI: 10.3390/cells8121625]
- 4 Wang Y, Dawson VL, Dawson TM. Poly(ADP-ribose) signals to mitochondrial AIF: a key event in parthanatos. *Exp Neurol* 2009; **218**: 193-202 [PMID: 19332058 DOI: 10.1016/j.expneurol.2009.03.020]
- 5 O'Sullivan J, Tedim Ferreira M, Gagné JP, Sharma AK, Hendzel MJ, Masson JY, Poirier GG. Emerging roles of eraser enzymes in the dynamic control of protein ADP-ribosylation. *Nat Commun* 2019; **10**: 1182 [PMID: 30862789 DOI: 10.1038/s41467-019-08859-x]
- 6 Harrison D, Gravells P, Thompson R, Bryant HE. Poly(ADP-Ribose) Glycohydrolase (PARG) vs. Poly(ADP-Ribose) Polymerase (PARP) - Function in Genome Maintenance and Relevance of Inhibitors for Anti-cancer Therapy. *Front Mol Biosci* 2020; **7**: 191 [PMID: 33005627 DOI: 10.3389/fmolb.2020.00191]
- 7 Jain A, Agostini LC, McCarthy GA, Chand SN, Ramirez A, Nevler A, Cozzitorto J, Schultz CW, Lowder CY, Smith KM, Waddell ID, Raites-Gurevich M, Stossel C, Gorman YG, Atias D, Yeo CJ, Winter JM, Olive KP, Golan T, Pishvaian MJ, Ogilvie D, James DI, Jordan AM, Brody JR. Poly (ADP) Ribose Glycohydrolase Can Be Effectively Targeted in Pancreatic Cancer. *Cancer Res* 2019; **79**: 4491-4502 [PMID: 31273064 DOI: 10.1158/0008-5472.CAN-18-3645]
- 8 Rossi A, Pizzo P, Filadi R. Calcium, mitochondria and cell metabolism: A functional triangle in bioenergetics. *Biochim Biophys Acta Mol Cell Res* 2019; **1866**: 1068-1078 [PMID: 30982525 DOI: 10.1016/j.bbamcr.2018.10.016]
- 9 Bertero E, Maack C. Calcium Signaling and Reactive Oxygen Species in Mitochondria. *Circ Res* 2018; **122**: 1460-1478 [PMID: 29748369 DOI: 10.1161/CIRCRESAHA.118.310082]
- 10 Pazzaglia S, Pioli C. Multifaceted Role of PARP-1 in DNA Repair and Inflammation: Pathological and Therapeutic Implications in Cancer and Non-Cancer Diseases. *Cells* 2019; **9** [PMID: 31877876 DOI: 10.3390/cells9010041]
- 11 Martí JM, Fernández-Cortés M, Serrano-Sáenz S, Zamudio-Martínez E, Delgado-Bellido D, García-Díaz A, Oliver FJ. The Multifactorial Role of PARP-1 in Tumor Microenvironment. *Cancers (Basel)* 2020; **12** [PMID: 32245040 DOI: 10.3390/cancers12071000]

- 10.3390/cancers12030739]
- 12 **Jeong KY**, Sim JJ, Park MH, Kim HM. Remodeling of Cancer-Specific Metabolism under Hypoxia with Lactate Calcium Salt in Human Colorectal Cancer Cells. *Cancers (Basel)* 2021; **13** [PMID: 33806179 DOI: 10.3390/cancers13071518]
- 13 **Hempel N**, Trebak M. Crosstalk between calcium and reactive oxygen species signaling in cancer. *Cell Calcium* 2017; **63**: 70-96 [PMID: 28143649 DOI: 10.1016/j.ceca.2017.01.007]
- 14 **Gupte R**, Liu Z, Kraus WL. PARPs and ADP-ribosylation: recent advances linking molecular functions to biological outcomes. *Genes Dev* 2017; **31**: 101-126 [PMID: 28202539 DOI: 10.1101/gad.291518.116]
- 15 **Perillo B**, Di Donato M, Pezone A, Di Zazzo E, Giovannelli P, Galasso G, Castoria G, Migliaccio A. ROS in cancer therapy: the bright side of the moon. *Exp Mol Med* 2020; **52**: 192-203 [PMID: 32060354 DOI: 10.1038/s12276-020-0384-2]
- 16 **Mashimo M**, Onishi M, Uno A, Tanimichi A, Nobeyama A, Mori M, Yamada S, Negi S, Bu X, Kato J, Moss J, Sanada N, Kizu R, Fujii T. The 89-kDa PARP1 cleavage fragment serves as a cytoplasmic PAR carrier to induce AIF-mediated apoptosis. *J Biol Chem* 2021; **296**: 100046 [PMID: 33168626 DOI: 10.1074/jbc.RA120.014479]
- 17 **Murata MM**, Kong X, Moncada E, Chen Y, Imamura H, Wang P, Berns MW, Yokomori K, Digman MA. NAD⁺ consumption by PARP1 in response to DNA damage triggers metabolic shift critical for damaged cell survival. *Mol Biol Cell* 2019; **30**: 2584-2597 [PMID: 31390283 DOI: 10.1091/mbc.E18-10-0650]
- 18 **Kassab MA**, Yu LL, Yu X. Targeting dePARylation for cancer therapy. *Cell Biosci* 2020; **10**: 7 [PMID: 32010441 DOI: 10.1186/s13578-020-0375-y]
- 19 **Liu L**, Li J, Ke Y, Zeng X, Gao J, Ba X, Wang R. The key players of parthanatos: opportunities for targeting multiple levels in the therapy of parthanatos-based pathogenesis. *Cell Mol Life Sci* 2022; **79**: 60 [PMID: 35000037 DOI: 10.1007/s00018-021-04109-w]
- 20 **Fatokun AA**, Dawson VL, Dawson TM. Parthanatos: mitochondrial-linked mechanisms and therapeutic opportunities. *Br J Pharmacol* 2014; **171**: 2000-2016 [PMID: 24684389 DOI: 10.1111/bph.12416]
- 21 **Randriamboavonjy V**, Kyselova A, Fleming I. Redox Regulation of Calpains: Consequences on Vascular Function. *Antioxid Redox Signal* 2019; **30**: 1011-1026 [PMID: 30266074 DOI: 10.1089/ars.2018.7607]
- 22 **Johnson DE**. Noncaspase proteases in apoptosis. *Leukemia* 2000; **14**: 1695-1703 [PMID: 10995018 DOI: 10.1038/sj.leu.2401879]



Published by **Baishideng Publishing Group Inc**
7041 Koll Center Parkway, Suite 160, Pleasanton, CA 94566, USA

Telephone: +1-925-3991568

E-mail: bpgoffice@wjgnet.com

Help Desk: <https://www.f6publishing.com/helpdesk>

<https://www.wjgnet.com>

